

# Elevated-temperature wear behaviors of NiMo/Mo<sub>2</sub>Ni<sub>3</sub>Si intermetallic “in situ” composites

Yongliang Gui, Chunyan Song,<sup>a)</sup> Shuhuan Wang, and Dingguo Zhao

College of Metallurgy and Energy, North China University of Science and Technology, Tangshan City, Hebei Province, 063009, People's Republic of China

(Received 22 June 2015; accepted 26 October 2015)

Intermetallic composite has been expected to be one kind of high-performance wear material at elevated temperature due to its inherent high hardness and strong atomic bonds. This paper presents the wear behaviors under elevated temperature conditions of NiMo/Mo<sub>2</sub>Ni<sub>3</sub>Si intermetallic “in situ” composite. Metallographic observations were carried out with optical microscope and scanning electron microscope. Elevated-temperature wear tests were performed under pin-on-disc mode dry sliding conditions. Results shown that the relative wear resistant property of NiMo/Mo<sub>2</sub>Ni<sub>3</sub>Si alloys at 500 °C is over 7 times, and become higher at 550 °C compared with austenitic 1Cr18Ni9Ti stainless steel. The effect of temperature and applied load on elevated-temperature wear resistance of alloy was evaluated. The corresponding wear mechanism is also reported through examining the worn surface, subsurface, and wear debris of the NiMo/Mo<sub>2</sub>Ni<sub>3</sub>Si intermetallic alloys which is found to be soft abrasive wear.



Yongliang Gui

Yongliang Gui was born in China on September 1979. He received Ph.D., degree in materials processing engineering from Beihang University (formerly name, Beijing University of Aeronautics and Astronautics), Beijing, China, in 2008, and the bachelor and master degrees in metallurgy engineering from North China University of Science and Technology, Tangshan, China, in 2000 and 2003, respectively.

In 2008, he joined the College of Metallurgy and Energy, North China University of Science and Technology, as a lecturer, and became an associate professor in 2010. His current research interests include intermetallic composite and novel metallic materials for wear application. Dr. Y.L. Gui is a fellow of Chinese Society for Metals and reviewer of many journals. He is a visiting fellow in Monash University, Australia, from December 2014 to December 2015 under the financial support of Chinese Scholarship Council.

He was the recipient of New Century 333 Talent Project third-level personnel of Hebei Province, China, in 2014, outstanding Supervisor of Graduate in North China University of Science and Technology, China, in 2013, Metallurgy Youth Award of Science and Technology of Hebei Province for his contributions to the field of metallurgy in 2012. He is currently the principal investigator of National Natural Science Foundation of China (1504087) and Natural Science Foundation-Steel and Iron Foundation of Hebei Province (E2014209213).

## I. INTRODUCTION

Many components, such as the barrels and screws of injection molding machines, mineral processing equipments, etc., are subjected to serious wear at elevated temperature. In some applications such as the nuclear, power generation, transport, and processing industries, etc., sliding wear of materials at high temperature is a critical problem because of the loss of strength of materials, and altered adhesion characteristics of the mating surfaces.

Intermetallic compounds usually exhibit outstanding wear resistance at elevated temperature conditions, and are emerg-

ing as a new group of advanced high-performance wear resistant candidate materials for many mechanical components working under aggressive tribological environments.<sup>1–6</sup> Among them, transition and refractory metal silicide are demonstrated to have better tribological properties because of not only their inherent high hardness and unique covalent–dominant strong atomic bonds but also abnormal hardness–temperature relation (higher hardness and strength at elevated temperature than those under ambient temperature).<sup>7–10</sup>

However, a relatively poor ductility and fracture toughness are currently a serious drawback restricting metal silicides from industrial applications,<sup>11,12</sup> but may be improved by suitable optimization of composite microstructures or use of innovative processing routes. A great deal of works on improvement of ductility and toughness has been carried out for binary refractory

Contributing Editor: Yang-T. Cheng

<sup>a)</sup>Address all correspondence to this author.

e-mail: scy@ncst.edu.cn

DOI: 10.1557/jmr.2015.348

metal-based metal silicides in Mo–Si, W–Si, and Nb–Si systems, and so on.<sup>13–15</sup> It is reported that ternary metal silicides exhibit better mechanical properties, compared to the binary metal silicides, because of their relatively weaker atomic bonding which provides good toughness at high hardness so as to become a promising reinforcement phase for wear resistant composites.<sup>16,17</sup>

Molybdenum nickel silicide Mo<sub>2</sub>Ni<sub>3</sub>Si, with a topologically closed packed (TCP) having the hP12 MgZn<sub>2</sub>-type Laves phase crystal lattice, has been proved to be a novel and potential high-temperature wear resistant material.<sup>18–20</sup> The inherent high hardness and insensitive temperature dependence guarantee Mo<sub>2</sub>Ni<sub>3</sub>Si outstanding abrasive wear resistance at elevated temperature and the strong mixed metallic-covalent atomic bonds provide excellent adhesive wear resistance and low friction coefficient to Mo<sub>2</sub>Ni<sub>3</sub>Si. Moreover, ternary metal silicide Mo<sub>2</sub>Ni<sub>3</sub>Si may further optimize the properties of binary intermetallic compounds in Mo–Si or Ni–Si system, offering good creep resistance at high temperature as well as relatively low density.

Compared to monolithic metal silicide alloys, multicomponent and multiphase intermetallic composite could have a better combination of toughness and strength.<sup>21–23</sup> As for the processing technique, “in situ” incorporation of ductile phases into metal silicide has been proved widely being an effective and practical way among all toughening means in an attempt to improve the ductility and fracture toughness metal silicides.<sup>24–26</sup> Our previous works have proved that NiMo/Mo<sub>2</sub>Ni<sub>3</sub>Si intermetallic “in situ” composites have

excellent wear resistance at ambient temperature.<sup>18</sup> However, the high-temperature wear resistant property and mechanism are still not clear for NiMo/Mo<sub>2</sub>Ni<sub>3</sub>Si intermetallic “in situ” composites. This paper primarily focuses on the evaluation of high-temperature wear resistance and subsequent discussion on the governing mechanisms by examining the worn surface, debris, and subsurface with scanning electron microscopes (SEM).

## II. EXPERIMENTAL PROCEDURES

The starting materials used for fabricating the NiMo/Mo<sub>2</sub>Ni<sub>3</sub>Si “in situ” intermetallic composites were commercial elemental powder of 99.9 wt% molybdenum, 99.5 wt% nickel, and 99.96 wt% silicon with the particle size ranging from 35 to 74 μm. The nominal chemical composition is 36Mo–48Ni–16Si (at.%) which is selected in the pseudo NiMo–Mo<sub>2</sub>Ni<sub>3</sub>Si binary system region in the isothermal section of Mo–Ni–Si ternary phase diagram at 1000 °C, as shown in Fig. 1. To produce the NiMo/Mo<sub>2</sub>Ni<sub>3</sub>Si alloys with homogeneous microstructure, all alloy ingots were remelted 3 times before metallographic characterization and wear test. Thirty NiMo/Mo<sub>2</sub>Ni<sub>3</sub>Si alloy ingots were prepared for microstructure characterization and elevated-temperature wear tests. The technical parameters for arc-melting process were taken according to previous works which are optimized to be electric current of 300 A, voltage of 10–12 V, and the pressure of 65 kPa.

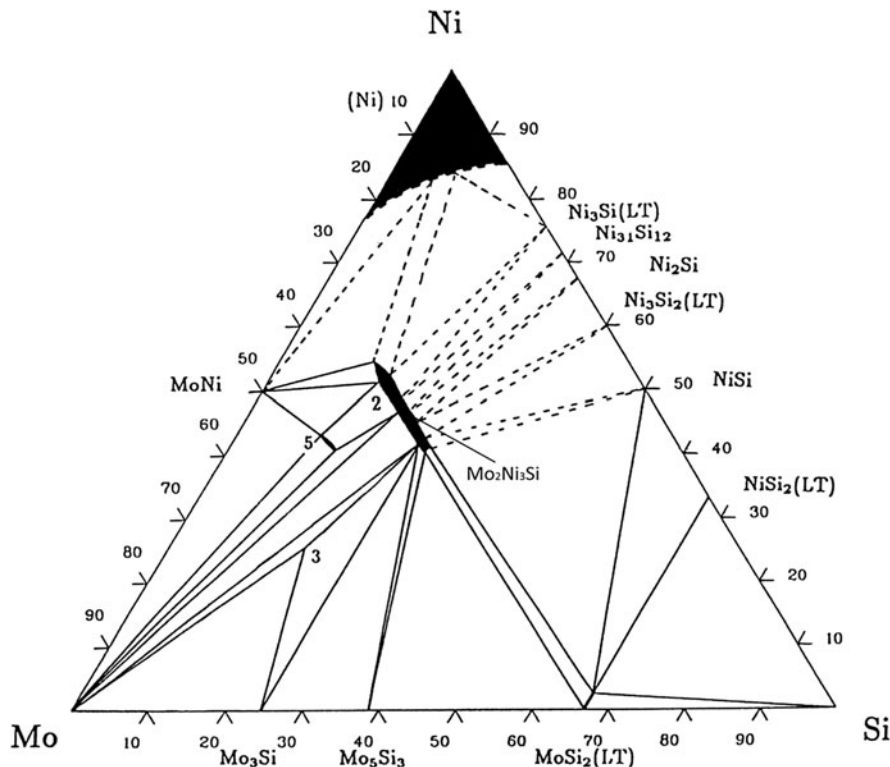


FIG. 1. Isothermal section of Mo–Ni–Si ternary phase diagram at 1000 °C.

Metallographic samples were prepared with standard mechanical polishing and chemical etching procedures. Microstructure of NiMo/Mo<sub>2</sub>Ni<sub>3</sub>Si “in situ” composites was characterized by AXIOVERT 200 MAT inverted optical microscope (Carl Zeiss Light Microscope GmbH, Göttingen, Germany) and KYKY-2800B SEM (KYKY Technology Development Ltd., Beijing, China). X-ray diffraction was carried on a D/MSX2500PC x-ray diffractometer (XRD; Rigaku Corporation, Tokyo, Japan) with Cu target K<sub>α</sub> radiation to determine the phase constituents of alloys. The specimens were scanned in the 2θ range of 20–80° in a scanning speed of 5°/min. Chemical compositions of each phase were analyzed with energy dispersive spectroscopy (EDS) equipped on KYKY-2800B SEM. Average hardness of the NiMo/Mo<sub>2</sub>Ni<sub>3</sub>Si alloys and the hardness of each composed phase was measured using a HXZ-1000 microhardness tester (Shanghai Optical Instrument Factory, Shanghai, China) with a load–dwell time of 15 s. The test load for hardness measurement is 500 g for average hardness of alloy and 200 g for hardness of phases, respectively.

Elevated-temperature wear property tests of the NiMo/Mo<sub>2</sub>Ni<sub>3</sub>Si “in situ” intermetallic composites were carried on a MG-2000 pin-on-disc mode (as shown in Fig. 2) wear testing machine with an electric furnace. The heating furnace is flexible to be opened in horizontal direction like a door for fixing and unfixing specimens and counterpart disc before and after tests. The pin-like specimens with a size of Φ6 mm × 10 mm (cylindrical shape) for wear test were cut from the alloy ingots by an electro-discharge

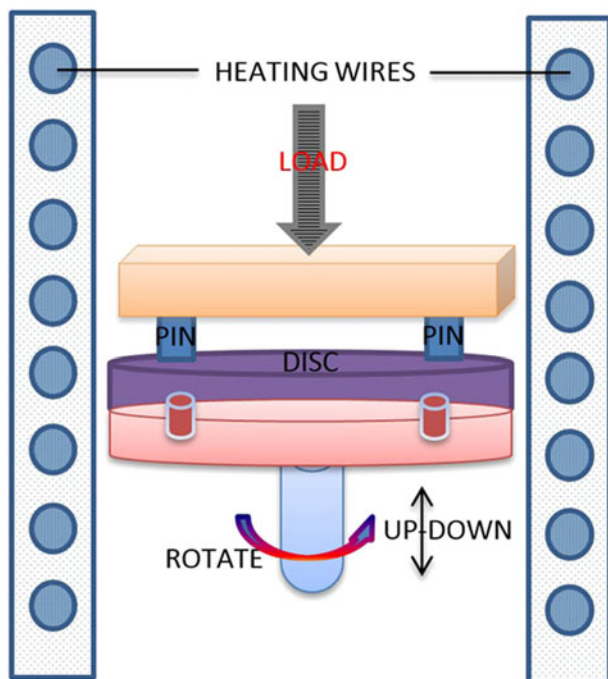


FIG. 2. Schematic illustration of pin-on-disc mode wear test at elevated temperature.

machine. The counterpart disc was made of solid-solution strengthened GH1015 Fe-based superalloy. The wear test parameters are as follows: total sliding distance of 174 m, wear test time of 30 min, sliding velocity of 0.097 m/s, test temperatures of 400, 450, 500 and 550 °C. In each wear test, two pin-like specimens of same alloy were simultaneously fixed on the contrary position of the specimen holder (indicated in Fig. 2) and active in the same wear track for the balance purpose. The normal applied loads of 49, 98, and 147 N resulted in the nominal contact pressure of 0.87, 1.73, and 2.60 MPa, respectively, for each test specimen.

The pin-shape alloy specimens and coupling disc were heated in electric furnace apart with a distance of 2 mm to avoid welding joint and adhesion with each other during heating process. When the temperature increased to test temperature, the counterpart disc was lifted up to the position where it contacts properly with alloy specimens. After that, the selected load was applied on the top and the mating disc started to rotate driven by an electric engine. To assess the wear resistance of the NiMo/Mo<sub>2</sub>Ni<sub>3</sub>Si at elevated temperature, the hot-rolled and solution-treated austenitic stainless steel 1Cr18Ni9Ti were selected as the reference materials for all wear test conditions. Wear mass loss of each test was measured using Sartorius BS110 electronic balance with an accuracy of 0.1 mg and the densities of the test materials were measured using the water immersion technique (i.e., Archimedes approach). Wear volume losses of all test were converted with the formula  $W_v = W_m/\rho$ , where  $W_v$  is the wear volume loss (mm<sup>3</sup>),  $W_m$  is the wear mass loss (mg), and  $\rho$  is the density (mg/mm<sup>3</sup>). Wear rates of the test materials were used as the index of wear resistance, which were calculated according to the expression  $W = W_v/L$ , where  $W$  is the wear rate (mm<sup>3</sup>/m),  $L$  is the sliding distance (m).

To explore the isothermal wear kinetics of NiMo/Mo<sub>2</sub>Ni<sub>3</sub>Si composite at elevated temperature, a cyclic wear test at 500 °C under a constant applied load of 98 N was performed. Both the test alloy specimens together with the specimen holder and coupling disc were disassembled and weighed in each 10 min interval, and then assembled again to go on successive wear test. Average result of three repeated tests was used to describe the isothermal wear kinetics. Finally, the morphologies of worn surface and wear debris, and subsurface microstructure were observed by KYKY-2800B SEM to assist in the analysis of corresponding wear mechanism.

### III. RESULTS

The specimens for microstructure observation were directly spark cut from the ingots after homogenization. Figure 3, shows SEM images of the NiMo/Mo<sub>2</sub>Ni<sub>3</sub>Si intermetallic “in situ” composites with the nominal chemical composition 36Mo–48Ni–16Si (at.%). The alloy ingots with a uniform and dense microstructure

consist of well-developed dendritic primary phase and long strip-like phase as well as certain amount of eutectic structure. It is interesting that the parallel long strip-like phase has obvious grown direction and nearly equal distance between two stripes, as shown in Fig. 3(a). According to the x-ray diffraction result, as shown in Fig. 4, it can be seen that the alloy is composed of two phases: binary intermetallic compound NiMo and ternary metal silicide Mo<sub>2</sub>Ni<sub>3</sub>Si based on the JCPDS file numbers 65-6903 and 15-0489. There is a little peak shift for both phases owing to the solid-solution of other elements during rapid solidification process. The EDS results showed that the average chemical compositions of primary dendrite phase and long stripe-like phase are Mo34.4Ni50.2Si15.4 (at.%) and Mo45.7Ni47.1Si7.2 (at.%), respectively.

It can be easily identified according to the XRD and EDS results that the primary dendritic phase is Mo-rich ternary metal silicide Mo<sub>2</sub>Ni<sub>3</sub>Si, a TCP structure with MgZn<sub>2</sub>-type Laves crystal lattice, and the long stripe-like phase with evident grow direction is intermetallic NiMo dissolving a certain amount of Si element. In the last solidification stage, as a result of continuous changing

chemical composition of liquid, the small amount of remaining residual liquid complete the phase transformation into solid in the form of eutectic crystallization of NiMo and Mo<sub>2</sub>Ni<sub>3</sub>Si.

The two constituent phases of intermetallic NiMo and Mo<sub>2</sub>Ni<sub>3</sub>Si with inherent high hardness imply NiMo/Mo<sub>2</sub>Ni<sub>3</sub>Si “in situ” composite has high average hardness. According to the detection results of HXZ-1000 microhardness tester, the average hardness of NiMo/Mo<sub>2</sub>Ni<sub>3</sub>Si alloy is up to HV1050. The hardness of distributed uniformly ternary metallic silicide Mo<sub>2</sub>Ni<sub>3</sub>Si phase is about HV1130 which is consistent with results in NiSi/Mo<sub>2</sub>Ni<sub>3</sub>Si alloys.<sup>19</sup> The volume fraction of primary Mo<sub>2</sub>Ni<sub>3</sub>Si dendrite in NiMo/Mo<sub>2</sub>Ni<sub>3</sub>Si alloys is approximately 65%. The density of the NiMo/Mo<sub>2</sub>Ni<sub>3</sub>Si alloy and comparing 1Cr18Ni9Ti stainless steel is 9.07 and 7.71 g/cm<sup>3</sup>, respectively, detected using Archimedes approach.

The measured wear mass losses, calculated wear volume losses, and wear rates of the NiMo/Mo<sub>2</sub>Ni<sub>3</sub>Si “in situ” intermetallic composite and reference material of 1Cr18Ni9Ti stainless steel with the applied load of 98 N and the test temperature of 500 °C are listed in Table I.

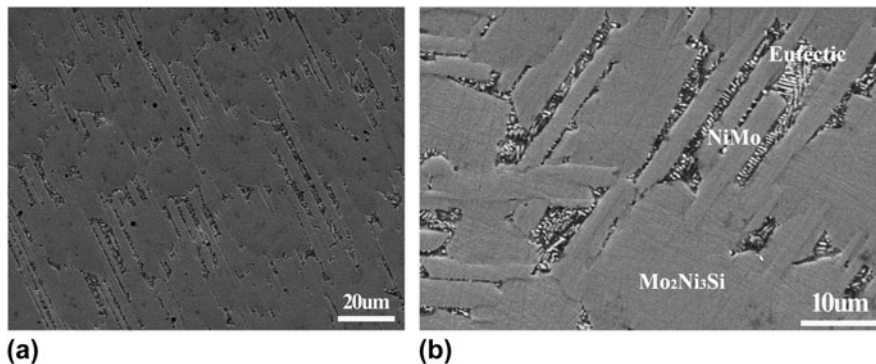


FIG. 3. Low (a) and high (b) magnification SEM micrographs showing microstructure of the NiMo/Mo<sub>2</sub>Ni<sub>3</sub>Si “in situ” composites.

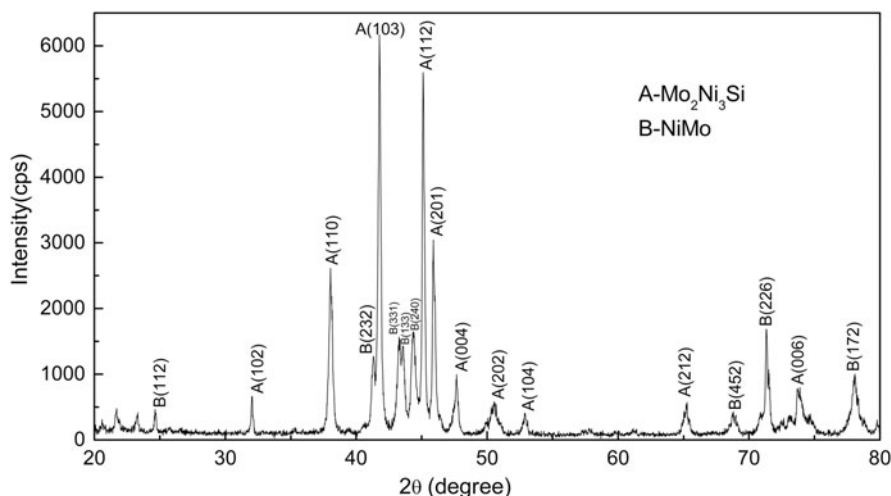


FIG. 4. X-ray diffraction patterns of the NiMo/Mo<sub>2</sub>Ni<sub>3</sub>Si “in situ” composites.

Inspection of Table I reveals that either wear mass or volume loss or wear rate of the NiMo/Mo<sub>2</sub>Ni<sub>3</sub>Si alloys are significantly lower than those of 1Cr18Ni9Ti stainless steel. The relative wear resistance is over seven times at 500 °C and even greater at 550 °C, as indicated in Fig. 5(a), compared with reference materials austenitic 1Cr18Ni9Ti stainless steel. Here the relative wear resistance refers to the ratio of wear rate between test material (NiMo/Mo<sub>2</sub>Ni<sub>3</sub>Si “in situ” intermetallic composite) and reference material (austenitic 1Cr18Ni9Ti stainless steel). Furthermore, the wear mass loss of coupling disc with the NiMo/Mo<sub>2</sub>Ni<sub>3</sub>Si alloy is much lower than with austenitic 1Cr18Ni9Ti stainless steel. It appears that the NiMo/Mo<sub>2</sub>Ni<sub>3</sub>Si alloy has excellent wear resistant and tribological compatibility under elevated-temperature dry sliding wear conditions.

According to the wear test results under different temperature and load, the wear rates of the NiMo/Mo<sub>2</sub>Ni<sub>3</sub>Si alloys under all test conditions are less than austenitic 1Cr18Ni9Ti stainless steels. As shown in Fig. 5(a), with the increasing temperature from 400 to 550 °C, the wear rate of 1Cr18Ni9Ti stainless steels increased from  $26.81 \times 10^{-3}$  to  $39.07 \times 10^{-3}$  mm<sup>3</sup>/m, while that of the NiMo/Mo<sub>2</sub>Ni<sub>3</sub>Si alloys decreased from  $6.02 \times 10^{-3}$  to  $4.25 \times 10^{-3}$  mm<sup>3</sup>/m. The wear mass and volume loss of the test alloys display same trend with the change of wear test temperature which means the NiMo/Mo<sub>2</sub>Ni<sub>3</sub>Si alloys have abnormal wear–temperature relationship. Moreover, under selected high-temperature wear test conditions, the variation of wear mass loss from three repeated tests is also considerably lower than those of reference materials. Figure 5(b), gives the effect of applied load on wear rate of test materials at 500 °C. It is clear that wear rate of the

NiMo/Mo<sub>2</sub>Ni<sub>3</sub>Si wear alloys increases very slowly compared with the tremendous increase of reference materials as the increases of applied load. It indicates that the NiMo/Mo<sub>2</sub>Ni<sub>3</sub>Si intermetallic composites have lower wear–load coefficient than reference material, austenitic 1Cr18Ni9Ti stainless steel, under high-temperature sliding wear conditions.

Figure 6 presented the results of cyclic wear in terms of wear rate, volumetric wear loss per unit wear distance, as a function of time during isothermal wear test of intermetallic NiMo/Mo<sub>2</sub>Ni<sub>3</sub>Si composite and coupling wear disc at 500 °C. The wear rate of both test alloy and mating disc follows a linear relationship with time, but in a different slope for the former 30 min and later half wear test time, as shown in Fig. 6. In the beginning 30 min, the slope was approximately 0.158, while it reduced to 0.066 for the next 30 min. The coupling of GH1015 Fe-based superalloy displayed a similar trend with the test NiMo/Mo<sub>2</sub>Ni<sub>3</sub>Si alloy.

All these wear test results provide strong evidences that the NiMo/Mo<sub>2</sub>Ni<sub>3</sub>Si in situ composites have outstanding wear resistance under elevated-temperature sliding wear condition with solid-solution strengthened GH1015 Fe-based superalloy as coupling wear material. The phenomenon suggests the NiMo/Mo<sub>2</sub>Ni<sub>3</sub>Si alloy keeps its high strength and hardness all along even at a higher temperature and applied load, and then is expected to be a type of promising and high-performance wear resistant material.

#### IV. DISCUSSION

Concomitant with the acceleration of wear rate is a difference in the material removal process and mechanism. To investigate the wear mechanism of the NiMo/

TABLE I. Wear test results of the NiMo/Mo<sub>2</sub>Ni<sub>3</sub>Si alloy specimens and reference material at 500 °C.

| Test material                                 | Wear mass loss (mg) |               | Wear volume loss (mm <sup>3</sup> ) | Wear rate (10 <sup>-3</sup> mm <sup>3</sup> /m) | Relative wear resistance |
|---|---------------------|---------------|-------------------------------------|---|--------------------------|
|   | Specimen            | Coupling disc |                                     |   |                          |
| NiMo/Mo <sub>2</sub> Ni <sub>3</sub> Si alloy | 7.1                 | 87.4          | 0.783                               | 4.50  | 7.16                     |
| 1Cr18Ni9Ti steel                              | 43.2                | 147.8         | 5.604                               | 32.21   | 1                        |

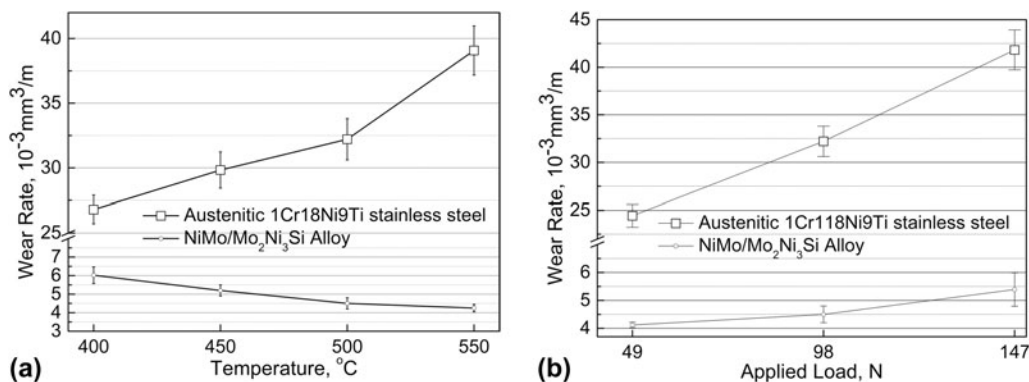


FIG. 5. Effect of (a) temperature and (b) load on wear rate of the NiMo/Mo<sub>2</sub>Ni<sub>3</sub>Si in situ composite and austenitic 1Cr18Ni9Ti stainless steel.

Mo<sub>2</sub>Ni<sub>3</sub>Si intermetallic composite, the worn surface, worn subsurface, and wear debris was examined using XRD and KYKY-2800B SEM.

The worn surfaces of the NiMo/Mo<sub>2</sub>Ni<sub>3</sub>Si intermetallic composite after a dry sliding wear test distance of 174 m at 500 °C with the load of 98 N are very smooth, typically shown in Fig. 7(a). No any obvious features of metallic adhesion and abrasive wear, i.e., grooves and plowing, are observed on the worn surface of NiMo/Mo<sub>2</sub>Ni<sub>3</sub>Si alloys.

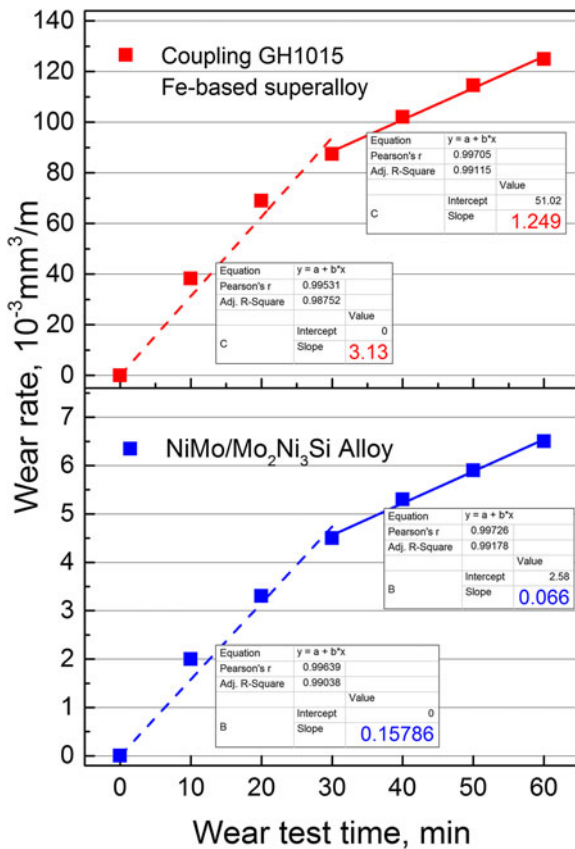


FIG. 6. Variation of the wear rate as a function of wear test time for the intermetallic NiMo/Mo<sub>2</sub>Ni<sub>3</sub>Si composite and coupling solid-solution strengthened GH1015 Fe-based superalloy disc during dry sliding wear process at 500 °C in air with the applied load of 98 N.

However, the morphologies of worn surface of the 1Cr18Ni9Ti stainless steels, with noticeable grooves and adhesion and deformation features, indicated that the materials were removed by abrasive wear accompanied by metallic adhesion with GH1015 Fe-based superalloy as the sliding-mating counterpart, as shown in Fig. 8.

The unique chemical and physical properties inherent to the ternary transition metal silicide Mo<sub>2</sub>Ni<sub>3</sub>Si and binary intermetallic NiMo as well as the uniform microstructure are the essential factors providing NiMo/Mo<sub>2</sub>Ni<sub>3</sub>Si intermetallic composites with outstanding wear resistant properties at elevated-temperature sliding wear conditions (as indicated in Fig. 5). As typical intermetallic phases, NiMo and Mo<sub>2</sub>Ni<sub>3</sub>Si have unique covalent-dominant strong atomic bonds which prevented effectively the NiMo/Mo<sub>2</sub>Ni<sub>3</sub>Si alloy on the wear contact surface from plastic deformation, adhesion and materials transferring as well as welding joint to the opposite surface of the sliding-coupling counterpart, metallic GH1015 superalloy asperities. Therefore, the two constitute phases, ternary metal silicide Mo<sub>2</sub>Ni<sub>3</sub>Si and binary intermetallic NiMo, played the critical role in resisting adhesive wear attacks in the process of elevated-temperature metallic sliding wear test. Both binary intermetallic NiMo and ternary metal silicide Mo<sub>2</sub>Ni<sub>3</sub>Si have high hardness and anomalous relation of hardness and temperature (hardness is stable or even increases with the increasing of temperature) which guarantee that the NiMo/Mo<sub>2</sub>Ni<sub>3</sub>Si alloy still has high hardness at the very contacting surface. It is a benefit to improve the abrasive wear resistant property of the NiMo/Mo<sub>2</sub>Ni<sub>3</sub>Si intermetallic composites at elevated temperatures, i.e., microcutting and microplowing, with GH1015 Fe-based superalloys as a coupling disc under applied pressure. These are demonstrated clearly from the very smooth worn surface of the NiMo/Mo<sub>2</sub>Ni<sub>3</sub>Si alloys where no characteristic features of metallic adhesion and abrasive wear are visible, as shown in Fig. 7.

In high-temperature sliding wear test process, due to the presence of normal stress from the top pin-like NiMo/Mo<sub>2</sub>Ni<sub>3</sub>Si alloy samples, coupling disc is subjected to the

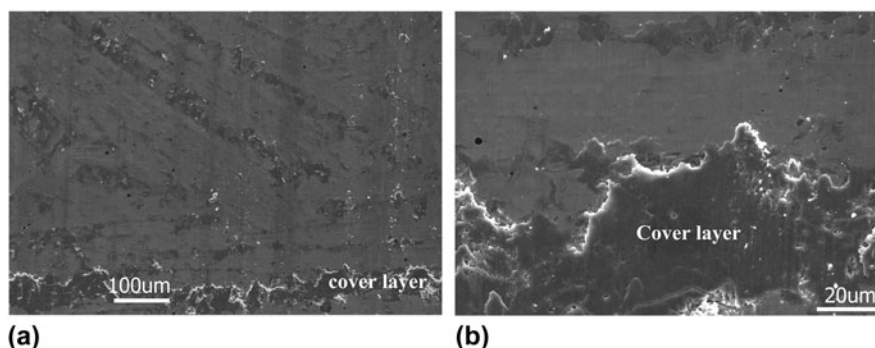


FIG. 7. Low (a) and high (b) magnification SEM micrographs illustrate worn surfaces of the NiMo/Mo<sub>2</sub>Ni<sub>3</sub>Si intermetallic composites.

repeated cyclic plastic deformation associated with a formation of deep parallel grooves along the sliding direction. In the meanwhile, coupling NiMo/Mo<sub>2</sub>Ni<sub>3</sub>Si intermetallic alloys with high hardness penetrate and plow deep into the surface of counterpart GH1015 superalloy disc under shearing stress and push to the ridges along the edges of the grooves. All these have caused the formation of deep and long grooves throughout the surface and extensive weight loss of the coupling disc and then materials were removed under the combined action of plowing, cutting, and fracture.

Generally, the Archard wear equation is a simple model used to describe isothermal sliding wear kinetics which is given as below:

$$W_v = K \cdot P \cdot s \quad (1)$$

where,  $W_v$ ,  $K$ ,  $P$ , and  $s$  are the volumetric wear loss, specific wear rate coefficient, normal applied load, and sliding wear distance, respectively. In the light of this, wear rate equation of the NiMo/Mo<sub>2</sub>Ni<sub>3</sub>Si intermetallic alloy, at the wear test condition with the temperature of 500 °C and actual contact load of 49 N (half of total normal applied load), could be predicted based on the test results in Fig. 6 to be as following:

$$\text{in the beginning 30 min, } W_v = 0.0271 \cdot s \quad (2)$$

$$\text{since 30 min, } W_v = 0.0113 \cdot s + 2.58 \quad (3)$$

where, the unit for  $W_v$  and  $s$  is mm<sup>3</sup>/m and m, respectively. It provides guidelines for service life prediction of the wear resistant intermetallic composites based on Mo–Ni–Si ternary system.

Wear debris generated during elevated-temperature wear test process was collected at the end of test and examined by XRD, SEM, and EDS to assist investigating the wear mechanisms. Figure 9 shows the SEM images of wear debris of the NiMo/Mo<sub>2</sub>Ni<sub>3</sub>Si intermetallic composite and the 1Cr18Ni9Ti austenitic stainless steel produced at the applied load of 98 N and test temperature of 500 °C. The wear debris of the NiMo/Mo<sub>2</sub>Ni<sub>3</sub>Si test alloy exhibited a size distribution from tiny powder and irregular shaped particulate to large sheet-like debris (up to 10–20 μm in size) as well as some loosely agglomerated powder clusters. For reference 1Cr18Ni9Ti austenitic stainless steel, the large sheet-like debris was dominant with size up to ~100 μm which was consistent with worn surface appearance (Fig. 8).

As shown in Fig. 10, the XRD result reveals that the wear debris of the NiMo/Mo<sub>2</sub>Ni<sub>3</sub>Si alloy at elevated-temperature

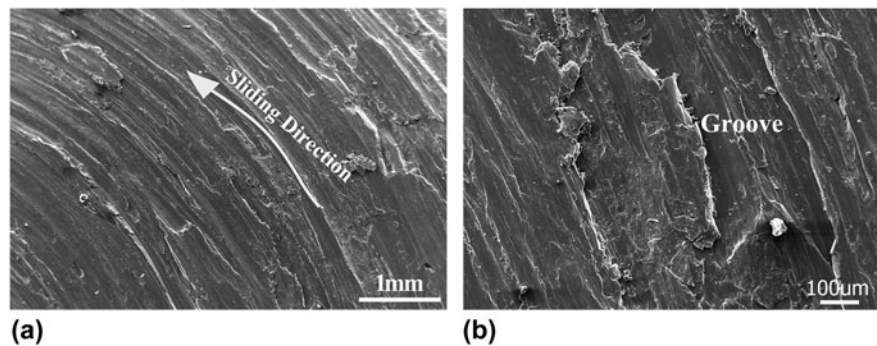


FIG. 8. Low (a) and high (b) magnification SEM micrographs showing the worn surfaces of the austenitic 1Cr18Ni9Ti stainless steel.

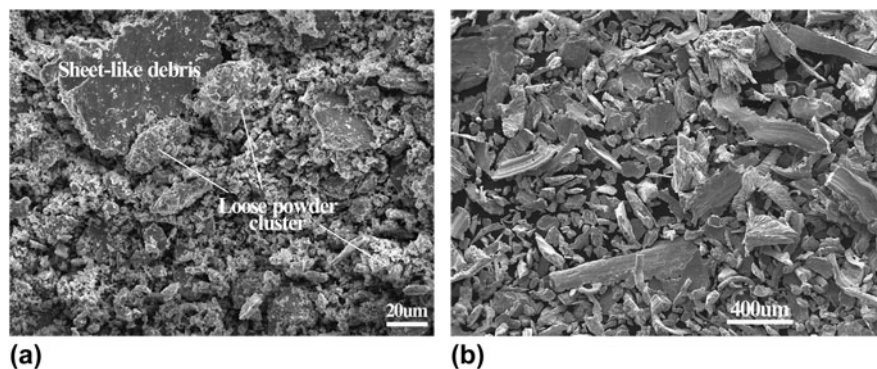


FIG. 9. SEM micrographs of wear debris of (a) the NiMo/Mo<sub>2</sub>Ni<sub>3</sub>Si intermetallic composite and (b) the reference austenitic stainless steel 1Cr18Ni9Ti at applied load of 98 N and temperature of 500 °C.

wear test conditions is a complex mixture of many phases including Fe<sub>2</sub>O<sub>3</sub>, Fe<sub>3</sub>O<sub>4</sub>, SiO<sub>2</sub>, Mo<sub>2</sub>Ni<sub>3</sub>Si, etc. Further EDS examination indicates that the chemical composition of the tiny powders and loosely agglomerated powder clusters are Fe56.74%Ni10.97%Mo7.12%Si3.23%O21.94%, and the large sheet-like debris is highly enriched in Fe with the chemical composition of Fe72.39%Ni3.03%Mo1.74%Si0.69%O22.15%. The tiny powder and loosely agglomerated powder clusters are identified as the complex oxides which are primarily originated from the contacting surface of mating GH1015 superalloy counterpart and secondarily from NiMo/Mo<sub>2</sub>Ni<sub>3</sub>Si alloy specimens. The agglomerated powder clusters were likely the assembly of lots of tiny wear powder under the pushing force of coupling wear pairs during wear process. The sheet-like debris is derived from following two sources: fracture directly from GH1015 superalloy disc due to adhesive and abrasive wear attack, and repeated rolling-consolidated product of tiny wear powder between the pin-like NiMo/Mo<sub>2</sub>Ni<sub>3</sub>Si alloy samples and GH1015 superalloy disc. In the meanwhile, it was implicated from the EDS results that oxidation reaction occurred in the process of elevated-temperature dry sliding wear tests.

Microstructure including shape, size, volume fraction, and distribution of constituent phases, together with hardness of materials is always related to wear resistant properties and plastic deformation. As shown in Fig. 11, serious plastic deformation occurred in the worn sub-surface of the reference test materials, solid-solution austenitic 1Cr18Ni9Ti stainless steel, whereas no evidence of local plastic deformation and selective wear to NiMo and Mo<sub>2</sub>Ni<sub>3</sub>Si phases was observed in the NiMo/Mo<sub>2</sub>Ni<sub>3</sub>Si intermetallic alloys. Generally speaking, metallic materials have the weaker atomic bonds resulting from the metallic bonding without mostly nondirectional.

This leads to the low plastic deformation resistance because the dislocation motions are easy to start and extend. However, for intermetallic composite with covalent bonds, the atomic bonding is directional in nature and hence the dislocation motion is difficult which increases the strength and plastic deformation resistance.

As well known, the existence of an oxidation scale on worn surface, formed at high-temperature open air, has a significant impact on the wear behavior and mechanism of metallic materials.<sup>27,28</sup> To confirm whether or not some oxidation layers formed on the worn surface of the NiMo/Mo<sub>2</sub>Ni<sub>3</sub>Si intermetallic composite at selected wear test temperature, we conducted an oxidation test of NiMo/Mo<sub>2</sub>Ni<sub>3</sub>Si alloy at 500 °C for 3 h. Result shows that the increase of weight was unable to be detected for a 2.56 g NiMo/Mo<sub>2</sub>Ni<sub>3</sub>Si alloy sample with the size of  $\phi 6 \text{ mm} \times 10 \text{ mm}$ , and the total gain in mass of three same alloy samples (10 mm  $\times$  10 mm  $\times$  10 mm in size) with the total weight of 27.21 g is only 0.1 mg. This result gives the mass gain per unit area which is 0.06  $\mu\text{g}/\text{mm}^2$  for the NiMo/Mo<sub>2</sub>Ni<sub>3</sub>Si alloy at 500 °C open air. The negligible gain in weight suggests that the oxidation reaction at wear test temperature is too weak to be taken into consideration of discussion on wear behaviors and mechanisms at the temperature around 500 °C. Further, the gain in weight is possibly the formation of a little SiO<sub>2</sub> oxidation scale by oxidation reaction.<sup>29,30</sup> This result also indicates that the SiO<sub>2</sub> layer formed may be quite thin in depth at around 500 °C, but must be adhere and spalling resistant enough to provide necessary protection against further oxidation of the underlying substrate.

It is necessary to note that some uneven and nonuniformly distributed cover layers especially some nearly continuous cover slips were discovered easily from the

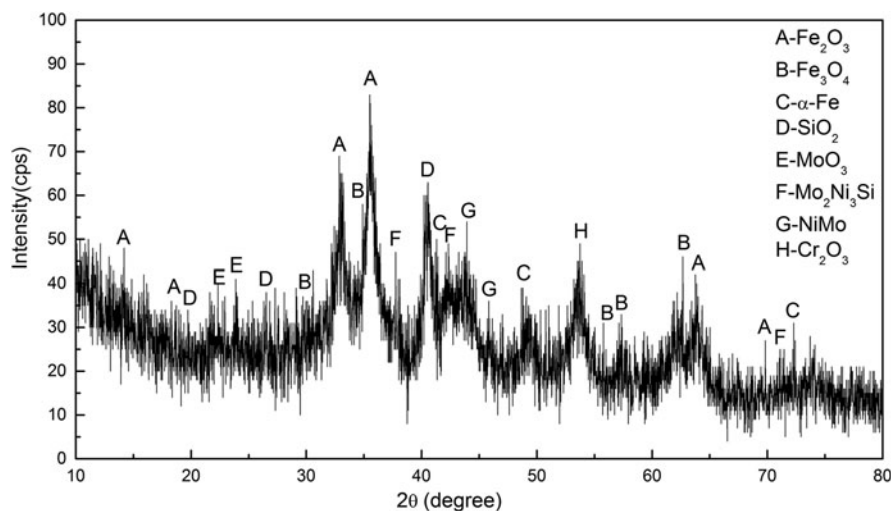


FIG. 10. XRD patterns of wear debris for NiMo/Mo<sub>2</sub>Ni<sub>3</sub>Si intermetallic composites at wear test condition with the test temperature of 500 °C and applied load of 98 N.

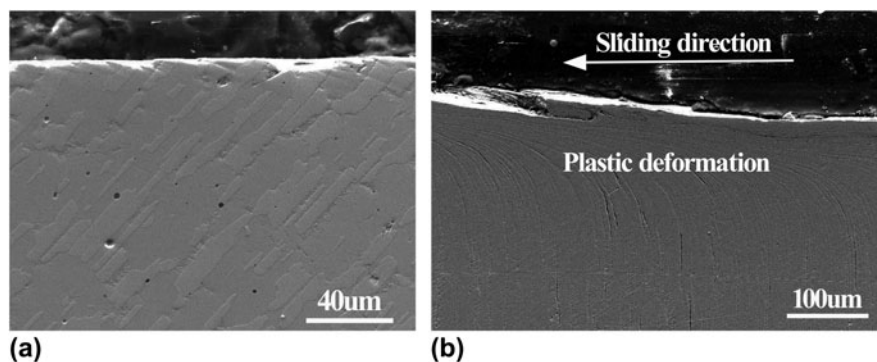


FIG. 11. SEM micrographs showing the worn subsurface morphology of (a) the NiMo/Mo<sub>2</sub>Ni<sub>3</sub>Si intermetallic composite and (b) the reference austenitic stainless steel 1Cr18Ni9Ti.

worn surfaces of the NiMo/Mo<sub>2</sub>Ni<sub>3</sub>Si intermetallic composites. From careful observation, it could be found that the cover layers are not an integral sheet-like metallic materials layer but accumulation of powders, as indicated in Fig. 7(b). The chemical composition of the cover layers is detected by EDS, which was found to be Fe55.58%Ni11.72%Mo8.64%Si4.17%O19.89%. This is highly consistent with the element constituents of loosely agglomerated powder clusters in wear debris.

When slide-coupling with the solid-solution strengthened GH1015 Fe-based superalloy rotating disc, the asperities on the contact surface of the NiMo/Mo<sub>2</sub>Ni<sub>3</sub>Si intermetallic composites were very difficult to be either plastically deformed due to its high hardness and hardness anomaly or adhered to the counterpart contacting surface owing to the strong covalent-dominant atomic bonds. On the contrary, the asperities of the mating softer Fe-based superalloy disc were inevitable to plastic deformation (Fig. 11), and are easily plowed and wore because of the relatively low hardness. As a consequence, wear debris mainly from Fe-based superalloy disc was produced. These wear debris clustered gradually and rolled back over the sliding contact surface of the NiMo/Mo<sub>2</sub>Ni<sub>3</sub>Si alloy specimen under repeated sliding interactions, leading to the formation of a cover layer. The cover layers were likely to enlarge or detach from the worn surface and newly form on other regions under the combined action of friction shearing, sliding-shearing, and repeated compression-rolling. Finally, the contact surface of the NiMo/Mo<sub>2</sub>Ni<sub>3</sub>Si alloy was partly covered by a transferred cover layer after the formation and detaching got a balance.

The presence of cover layers on the worn surface has some positive contribution to wear resistant property of the NiMo/Mo<sub>2</sub>Ni<sub>3</sub>Si alloys. On the one hand, the cover of transferred layer on contact surface prevents the NiMo/Mo<sub>2</sub>Ni<sub>3</sub>Si alloys from direct touch with mating wear disc, which reduce the chances of adhesive wear. On the other hand, the direct wear strikes from contact surface of coupling wear disc were avoided and then

enhance the abrasive wear resistance of NiMo/Mo<sub>2</sub>Ni<sub>3</sub>Si alloy since partial contact surfaces of NiMo/Mo<sub>2</sub>Ni<sub>3</sub>Si alloys are not exposed to coupling wear disc.

In summary, the high Fe content in cover layers and wear debris immediately illustrates that the wear debris is mainly from the counterpart disc GH1015 Fe-based superalloy with lower hardness and strength. This is also proved by the very low wear mass loss of NiMo/Mo<sub>2</sub>Ni<sub>3</sub>Si alloys and high wear mass loss of coupling disc listed in Table I. The smooth worn surface with the absence of plowing and worn subsurface without plastic deformation and selective wear clearly confirms that the NiMo/Mo<sub>2</sub>Ni<sub>3</sub>Si intermetallic composites keep high strength and hardness in nature and subsequently extraordinary high-temperature wear resistance. Therefore, the dominated wear mechanisms of the NiMo/Mo<sub>2</sub>Ni<sub>3</sub>Si intermetallic “in situ” composites under elevated-temperature dry sliding wear conditions are soft abrasive wear.

## V. CONCLUSIONS

The elevated-temperature wear behaviors of a novel wear resistant NiMo/Mo<sub>2</sub>Ni<sub>3</sub>Si intermetallic “in situ” composite, with a microstructure of primary dendritic Mo<sub>2</sub>Ni<sub>3</sub>Si ternary metal silicide and long stripe-like NiMo binary intermetallic phase with evident growing direction, was evaluated. Within the set of elevated-temperature wear conditions, the effect of temperature and load on the wear resistance, and wear mechanism of the NiMo/Mo<sub>2</sub>Ni<sub>3</sub>Si intermetallic “in situ” composites was obtained. The NiMo/Mo<sub>2</sub>Ni<sub>3</sub>Si alloys display remarkable property at high-temperature dry sliding wear test conditions and sluggish wear-load feature due to its high hardness and strong atomic bond. It is interesting that the NiMo/Mo<sub>2</sub>Ni<sub>3</sub>Si alloys exhibit amazing wear-temperature relation at temperature ranging from 400 to 550 °C. The NiMo/Mo<sub>2</sub>Ni<sub>3</sub>Si alloys are removed and wear mainly with the form of soft abrasive wear in the process of elevated-temperature dry sliding wear environments.

## ACKNOWLEDGMENTS

The authors are grateful to National Natural Science Foundation of China (51404087) and Natural Science Foundation-Steel and Iron Foundation of Hebei Province (E2014209213) for the financial support of this work. One of the authors (Y.L. Gui) wishes to thank Chinese Scholarship Council, for the financial support on his one-year visit in Monash University as a visiting fellow.

## REFERENCES

- J. Mu, P.F. Sha, Z.W. Zhu, Y.D. Wang, H.F. Zhang, and Z.Q. Hu: Synthesis of high strength aluminum alloys in the Al-Ni-La system. *J. Mater. Res.* **29**(5), 708 (2014).
- X.H. Zhang, J.Q. Ma, L.C. Fu, S.Y. Zhu, F. Li, J. Yang, and W.M. Liu: High temperature wear resistance of Fe-28Al-5Cr alloy and its composites reinforced by TiC. *Tribol. Int.* **61**, 48 (2013).
- M.S. Yang, X.B. Liu, J.W. Fan, X.M. He, S.H. Shi, G.Y. Fu, M.D. Wang, and S.F. Chen: Microstructure and wear behaviors of laser clad NiCr/Cr<sub>3</sub>C<sub>2</sub>-WS<sub>2</sub> high temperature self-lubricating wear-resistant composite coating. *Appl. Surf. Sci.* **258**(8), 3757 (2012).
- A.M.S. Malafaia, M.T. Milan, M. Omar, R.M.M. Riofano, and M.F. de Oliveira: Oxidation and abrasive wear of Fe-Si and Fe-Al intermetallic alloys. *J. Mater. Sci.* **45**(19), 5393 (2010).
- Z.H. Tang, A.J. Thom, M.J. Kramer, and M. Akinc: Characterization and oxidation behavior of silicide coating on multiphase Mo-Si-B alloy. *Intermetallics* **16**(9), 1125 (2008).
- D.K. Mu, J. Read, Y.F. Yang, and K. Nogita: Thermal expansion of Cu<sub>6</sub>Sn<sub>5</sub> and (Cu,Ni)<sub>6</sub>Sn<sub>5</sub>. *J. Mater. Res.* **26**(20), 2660 (2011).
- E. Koraman, M. Baydogan, S. Sayilgan, and A. Kalkanli: Dry sliding wear behaviour of Al-Fe-Si-V alloys at elevated temperatures. *Wear* **322**, 101 (2015).
- P. Mandal, A.J. Thom, M.J. Kramer, V. Behrani, and M. Akinc: Oxidation behavior of Mo-Si-B alloys in wet air. *Mater. Sci. Eng., A* **371**(1–2), 335 (2004).
- B.A. Gnesin, I.B. Gnesin, and A.N. Nekrasov: The silicide coatings (Mo,W)Si<sub>2</sub>+(Mo,W)<sub>5</sub>Si<sub>3</sub> on graphite, interaction with carbon. *J. Alloys Compd.* **549**, 308 (2013).
- W.Y. Kim, H. Tanaka, and S. Hanada: High temperature strength at 1773 K and room temperature fracture toughness of Nb<sub>55</sub>/Nb<sub>5</sub>Si<sub>3</sub> in situ composites alloyed with Mo. *J. Mater. Sci.* **37**(14), 2885 (2002).
- A.P. Alur and K.S. Kumar: Monotonic and cyclic crack growth response of a Mo-Si-B alloy. *Acta Mater.* **54**(2), 385 (2006).
- J-H. Kim, T. Tabaru, M. Sakamoto, and S. Hanada: Mechanical properties and fracture behavior of an Nb<sub>55</sub>/Nb<sub>5</sub>Si<sub>3</sub> in-situ composite modified by Mo and Hf alloying. *Mater. Sci. Eng., A* **372**(1–2), 137 (2004).
- M.Z. Alam, S. Saha, B. Sarma, and D.K. Das: Formation of WS<sub>2</sub> coating on tungsten and its short-term cyclic oxidation performance in air. *Int. J. Refract. Met. Hard Mater.* **29**(1), 54 (2011).
- S.K. Varma, C. Parga, K. Amato, and J. Hernandez: Microstructures and high temperature oxidation resistance of alloys from Nb-Cr-Si system. *J. Mater. Sci.* **45**(14), 3931 (2010).
- F. Maglia, C. Milanese, U. Anselmi-Tamburini, and Z.A. Munir: Self-propagating high-temperature synthesis microalloying of MoSi<sub>2</sub> with Nb and V. *J. Mater. Res.* **18**(8), 1842 (2003).
- S.H. Ha, K. Yoshimi, J. Nakamura, T. Kaneko, K. Maruyama, R. Tu, and T. Goto: Experimental study of Mo<sub>55</sub>-T<sub>2</sub>, Mo<sub>55</sub>-Mo<sub>3</sub>Si-T<sub>2</sub>, and Mo<sub>3</sub>Si-T<sub>2</sub> eutectic reactions in Mo-rich Mo-Si-B alloys. *J. Alloys Compd.* **594**, 52 (2014).
- D.Z. Wang, Q.W. Hu, and X.Y. Zeng: Microstructures and performances of Cr<sub>13</sub>Ni<sub>5</sub>Si<sub>2</sub> based composite coatings deposited by laser cladding and laser-induction hybrid cladding. *J. Alloys Compd.* **588**, 502 (2014).
- Y.L. Gui, C.Y. Song, L. Yang, and X.L. Qin: Microstructure and tribological properties of NiMo/Mo<sub>2</sub>Ni<sub>3</sub>Si intermetallic “in-situ” composites. *J. Alloys Compd.* **509**(15), 4987 (2011).
- X.D. Lu and H.M. Wang: Dry sliding wear behavior of laser clad Mo<sub>2</sub>Ni<sub>3</sub>Si/NiSi metal silicide composite coatings. *Thin Solid Films* **472**(1–2), 297 (2005).
- Y.L. Gui, X.J. Qi, and C.Y. Song: Metallic tribological compatibility of Mo<sub>55</sub>-toughened Mo<sub>2</sub>Ni<sub>3</sub>Si metal silicide alloys. In *Physical and Numerical Simulation of Material Processing VI*, (Jitai Nui, Guangtao Zhou, eds.; Zurich, Switzerland: Trans Tech Publications, 2011), p. 1068.
- R. Mitra: Mechanical behaviour and oxidation resistance of structural silicides. *Int. Mater. Rev.* **51**(1), 13 (2006).
- D. Van Heerden, A.J. Gavens, P.R. Subramanian, T. Foecke, and T.P. Weihs: The stability of Nb/Nb<sub>5</sub>Si<sub>3</sub> microlaminates at high temperatures. *Metall. Mater. Trans. A* **32**(9), 2363 (2001).
- A. Hekmat-Ardakan, F. Ajersch, and X.G. Chen: Microstructure modification of Al-17%Si alloy by addition of Mg. *J. Mater. Sci.* **46**(7), 2370 (2011).
- K. Niihara and Y. Suzuki: Strong monolithic and composite MoSi<sub>2</sub> materials by nanostructure design. *Mater. Sci. Eng., A* **261**(1–2), 6 (1999).
- R. Mitra, A.K. Srivastava, N.E. Prasad, and S. Kumari: Microstructure and mechanical behaviour of reaction hot pressed multiphase Mo-Si-B and Mo-Si-B-Al intermetallic alloys. *Intermetallics* **14**(12), 1461 (2006).
- C.L. Ma, J.G. Li, Y. Tan, R. Tanaka, and S. Hanada: Microstructure and mechanical properties of Nb/Nb<sub>5</sub>Si<sub>3</sub> in situ composites in Nb-Mo-Si and Nb-W-Si systems. *Mater. Sci. Eng., A* **386**(1–2), 375 (2004).
- J.D. Majumdar, B.L. Mordike, and I. Manna: Friction and wear behavior of Ti following laser surface alloying with Si, Al and Si plus Al. *Wear* **242**(1–2), 18 (2000).
- D. Roy, S. Kumari, R. Mitra, and I. Manna: Microstructure and mechanical properties of mechanically alloyed and spark plasma sintered amorphous-nanocrystalline Al(65)Cu(20)Ti(15) intermetallic matrix composite reinforced with TiO<sub>2</sub> nanoparticles. *Intermetallics* **15**(12), 1595 (2007).
- J.D. Majumdar, B.L. Mordike, S.K. Roy, and I. Manna: High-temperature oxidation behavior of laser-surface-alloyed Ti with Si and Si plus Al. *Oxid. Met.* **57**(5–6), 473 (2002).
- J.D. Majumdar, A. Weisheit, B.L. Mordike, and I. Manna: Laser surface alloying of Ti with Si, Al and Si plus Al for an improved oxidation resistance. *Mater. Sci. Eng., A* **266**(1–2), 123 (1999).